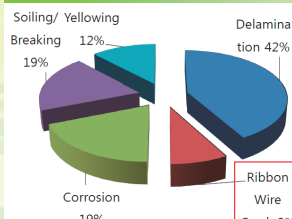


鈴木 聡^{1,2}, 棚橋 紀悟³, 土井 卓也³, 増田 淳³

¹太陽光発電技術研究組合, ²エスペック株式会社, ³国立研究開発法人 産業技術総合研究所

INTRODUCTION



Purpose
In this study, we tried to evaluate the sorting test for the breakage of ribbon for extracting the weak point or the defect inherent in the modules.

Changwon, H. et al., 2012 "Lifetime prediction of silicon PV module ribbon wire in three local weathers". NREL 2012 Photovoltaic Module Reliability Workshop.

MATERIALS AND METHOD



Figure 1. Photographs of load cycle bending machine.



Figure 2. Image of 4 point stress.

Table 1. Specifications of materials used in PV module.

Material	Specification	Supplier
Cell	Multicrystalline-Si cell (156 mm×156 mm)	Q Cells
Glass	Semi-tempered glass	AGC
Encapsulant	EVA	Nondisclosure
Interconnector	A-SPS (Leaded, Ag)	Hitachi Cable
Back sheet	PVF / PET / PVF	Nondisclosure
Size	540 mm × 200 mm × 4 mm	-



Figure 3. Photograph of PV module sample.

Table 2. Test conditions.

Stress	500 N
Bending / unbending	4 s / 4 s
Bending cycle	10,000 times each test
Temperature	-20°C / 25°C / 80°C

SIMULATION

Table 3. Materials properties used in simulation.

Size	540 mm × 200 mm × 4 mm
Young's modulus	73 GPa (7.3×10 ¹⁰ N/mm ²)
Poisson's ratio	0.21
Specific gravity	2.50 g/cm ³ (2.40×10 ⁻³ N/mm ³)

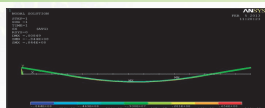


Figure 4. Results of 4 point bending test.

In order to estimate the suitable stress condition in the load cycle bending test, simulation was made by assuming that the property of glass represents those of PV modules. From the results of simulation as shown in Fig. 4, the maximum displacement was calculated to 8.5 mm with the stress of 500 N.

Table 4. Materials properties used in simulation at 23°C.

Unit	Glass	Silicon	EVA	PET	Copper	Solder
Young's modulus	Pa	7.31E+10	1.31E+11	1.68E+07	1.60E+06	1.30E+11
Poisson's ratio	-	0.22	0.27	0.45	0.33	0.34
Thermal expansion coefficient	1/°C	9.03E-06	4.15E-06	2.70E-04	2.50E-05	1.70E-05
density	g/cm ³	2.5	2.33	0.95	1.4	-

Table 5. Young's modulus of EVA.

Temperature (°C)	-20	23	80
Young's modulus (Pa)	1.40E+08	1.68E+07	1.03E+06

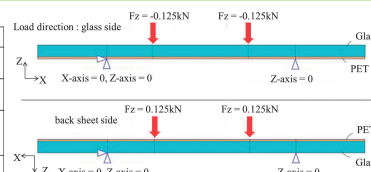


Figure 5. Boundary condition of simulation.

RESULTS & DISCUSSION

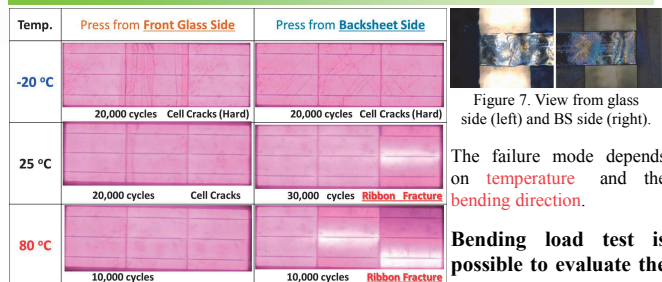


Figure 6. EL images after 4 point load cycle bending test.

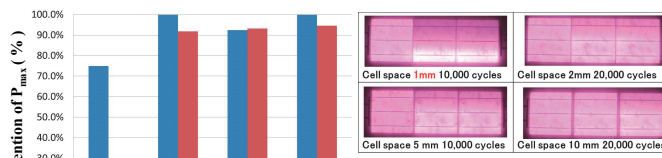


Figure 8. Retention of P_{max} after test of module with each cell space.

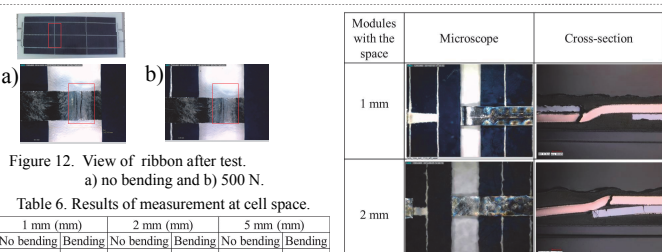


Figure 13. Microscopic view and cross section image.

Bending load test induces the breakage of ribbon.

SUMMARY

In this study, the following results were obtained:

1. Bending load test is useful for evaluating the breakage of ribbon.
2. The space over 1 mm between the cells is needed for high reliability.
3. The stress point of bending load concentrates on the interconnector and bending load tests are in close agreement with FEM simulations, but the estimated values by simulation are smaller than those by measurements.

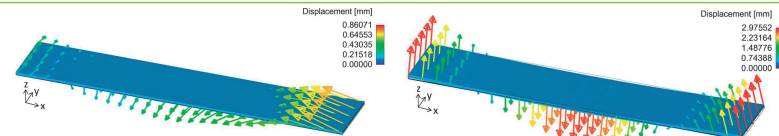


Figure 10. Results of FEM simulation of thermal stress (left) and bending load (right) from glass side at -20°C.

Bending load is more dominant than the thermal stress.

Temp.	Press from Front Glass Side	Press from Backsheet Side
-20 °C	386 -> 879 MPa (2.27-folds)	385 -> 878 MPa (2.28-folds)
23 °C	267 -> 438 MPa (1.64-folds)	267 -> 543 MPa (2.03-folds)
80 °C	306 -> 544 MPa (1.77-folds)	305 -> 1,065 MPa (3.49-folds)

Figure 11. Results of the maximum stress point of interconnector.

Bending load concentrates on the interconnector by the stress at 23°C and 80°C.

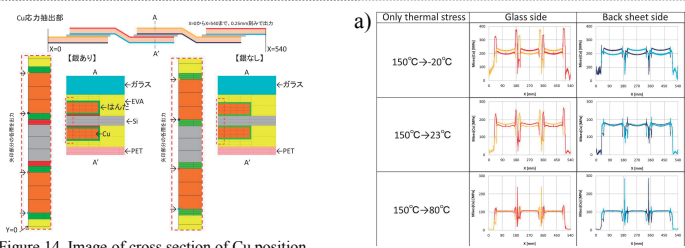


Figure 14. Image of cross section of Cu position.

Table 7. Comparison of displacement of modules between measurement and simulation.

Measurement (mm)	Glass side (mm)		Back sheet side (mm)	
	Only thermal stress	Bending load	Only thermal stress	Bending load
4.64	0.64	2.96	0.69	2.51
4.95	0.58	3.27	0.65	2.45
5.65	0.23	3.86	0.16	3.65

The evaluation values by simulation is smaller than those by the measurement.

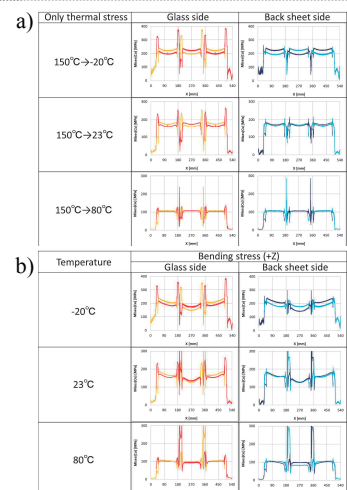


Figure 15. Stress distribution of Cu. a) thermal stress and b) bending load.